

Estimation of Energy Flux and Biomass in Pasture Areas through Remote Sensing Techniques

Ricardo Guimarães Andrade, Marcos Cicarini Hott, Walter Coelho Pereira Magalhães Junior

Brazilian Agricultural Research Corporation – Juiz de Fora, MG - Brazil

Abstract— Pasture production is estimated through remote sensing techniques with the aid of models and algorithms. The application with no need for extensive field measurements is one of the advantages of the Surface Energy Balance Algorithm for Land (SEBAL). The objective of this work was to estimate energy fluxes and, subsequently, pasture biomass with the aid of remote sensing techniques. The study area is located on the Experimental Farm of Embrapa Beef Cattle, municipality of Campo Grande, State of Mato Grosso do Sul, Brazil. For the implementation of the SEBAL and estimation of energy fluxes and biomass of the pasture areas, meteorological data and Landsat 5 - TM image were used. It was found that the technique has the potential to be applied to indicate the forage availability and to support decision-making in the planning and management of the extensive production of beef and milk cattle, with economic and environmental sustainability of pasture areas.

Keywords— geotechnology, livestock, SEBAL, sustainability, rural planning.

I. INTRODUCTION

The growing demand for food further reinforces the importance of increasing production with economic and environmental sustainability. Vilela et al. [1] have reported that intensifying and enhancing the efficiency of production systems may help to harmonize these interests. Hence, the sustainable use of pastures is a strategic issue, since most pasture areas are show some indication of degradation. The recovery of these areas may reduce the pressure for the opening of new farming and livestock frontiers, as well as contributing to diminishing the emission of greenhouse gases [2].

According to Dias-Filho [3], the support capacity would be the most flexible indicator to quantify the degradation of a given pasture. Currently, the only official parameter that is related to support capacity is the pasture stocking rate. This parameter has been presented by DIEESE [4],

and it is the result of the division of the number of animals by the area occupied by pastures of a given geographical unit. However, Dias-Filho [5] warns that a priori, it is not possible to guarantee the degradation condition of pasture only by evaluating its instantaneous support capacity (maximum number of animals supported by pasture, with no harm to pasture and to the animal).

Studies such as that carried out by Grigera et al. [6] highlight the potential of remote sensing techniques as a tool to assist in the implementation of systems for monitoring pasture production that makes it possible to identify, for example, the areas that require the adoption of acceptable management practices. Thus, models and algorithms are used to estimate pasture production using remote sensing techniques. One of these algorithms is the SEBAL (*Surface Energy Balance Algorithm for Land*) that was developed by Bastiaanssen et al. [7, 8].

One of the advantages of SEBAL is the flexibility in its structure so that other models can be coupled [9], facilitating the applications in studies carried out at a local and regional scale, with no need for extensive field measurements (Andrade et al. [10]). In order to estimate the above-ground biomass, Bastiaanssen and Ali [11] and Samarasinghe [12], among others, obtained good results by coupling the model of biomass accumulation proposed by Monteith [13] in the SEBAL associated with the model of efficiency use of the radiation that was structured by Field et al. [14]. As a result, the objective of this study was to estimate energy fluxes and, therefore, pasture biomass through the application of remote sensing techniques.

II. MATERIAL AND METHODS

The study area is located in the Experimental Farm of Embrapa Beef Cattle, municipality of Campo Grande, state of Mato Grosso do Sul, Brazil (Figure 1). According to the climatic classification of Köppen, the region is situated in a transition zone between humid temperate climate with hot summer (Cfa) and tropical climate with

dry winter season (Aw). The average annual temperature is 22.8°C, and the average annual rainfall is around 1,500 mm. The months with the lowest rainfall are June, July, and August. The soil in the study area is Red Latosol

Dystrophic class whose characteristic is a clayey texture, acid pH, low base saturation and high aluminum concentration [15].

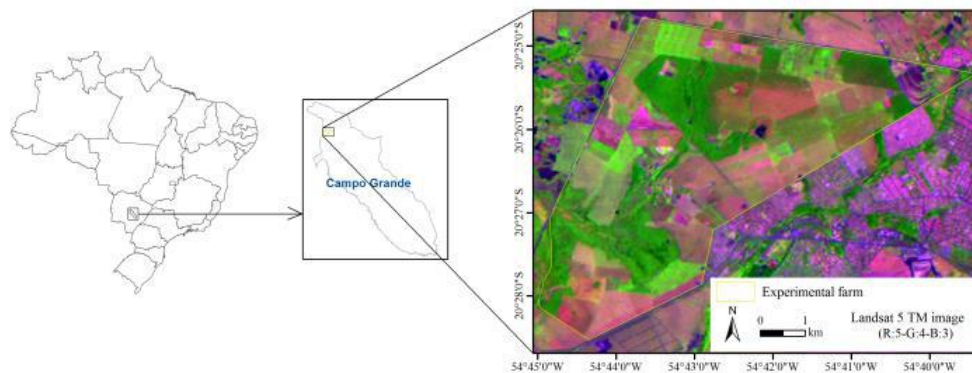


Fig. 1. Visualization of Experimental Farm of Embrapa Beef Cattle, municipality of Campo Grande, state of Mato Grosso do Sul, Brazil.

Meteorological data (air temperature, radiation, and wind speed) from the National Institute of Meteorology were obtained from meteorological station, latitude 20.45°S, longitude 54.6166°W and 530 meters above sea level in the municipality of Campo Grande, state of Mato Grosso do Sul, Brazil and from Landsat 5 - TM image of 12/21/2003 that has spatial resolution of 30 m at bands 1, 2, 3, 4, 5 and 7, and of 120 m in band 6 (thermal), acquired through the image catalog of the National Institute of Space Research - INPE, when accessing the site <http://www.dgi.inpe.br/CDSR/>.

The algorithm SEBAL was applied by using the data to estimate the components of the energy fluxes from pixel by pixel. In this case, the latent heat flux component was estimated as a residue of the other components of the energy balance, according to equation [7]:

$$LE = Rn - H - G$$

Where LE is the latent heat flux, Rn is the radiation balance, H is the sensible heat flux, and G is the soil heat flux, all in W m⁻². The radiation balance (Rn) was the first variable of the energy balance equation to be obtained. In this case, the equation suggested by Allen et al. [9] was applied:

$$Rn = R_{s\downarrow} - \alpha R_{s\downarrow} + R_{L\downarrow} - R_{L\uparrow} - (1 - \epsilon_o) R_{L\downarrow}$$

Where, R_{s↓} is the short-wave incident radiation (W m⁻²), R_{L↓} is the longwave radiation emitted by the atmosphere in the direction of the surface (W m⁻²), R_{L↑} is the longwave radiation emitted in the direction of the atmosphere (W m⁻²) and ε_o is the emissivity of the surface (dimensionless), α is the surface albedo (dimensionless). Allen et al. [9] show in detail the procedures involved in obtaining Rn.

After the calculation of Rn, the empirical equation suggested by Bastiaanssen [16] was used to estimate the soil heat flux (G, W m⁻²), given by:

$$G = \left[\frac{T_s}{\alpha} (0.0038\alpha + 0.0074\alpha^2)(1 - 0.98NDVI^4) \right] Rn$$

Where, T_s is the surface temperature (°C), α is the surface albedo (dimensionless), NDVI is the Normalized Difference Vegetation Index and Rn is the radiation balance. In order to correct the soil heat flux values for water bodies (NDVI < 0), G = 0.3Rn was considered [17]. Once the value of G was obtained, a new series of steps was started to obtain the sensible heat flux (H).

For the estimation of H, the process started by considering the neutral atmosphere condition. Firstly, the expressions suggested by Allen et al. [9] to obtain the initial roughness parameter (z_{om initial}), the initial friction velocity (u*_{initial}), the wind velocity at a height (z) of 100 m (blending height), where it is assumed that the surface roughness effects are negligible) and the initial aerodynamic drag (τ_{ah initial}). The roughness parameter (z_{om}) obtained as a function of SAVI (Soil Adjusted Vegetation Index) was used in the following steps.

SEBAL uses two pixels termed “anchor pixels” to set boundary conditions for the energy balance. These pixels are denominated “hot” and “cold” and located in the study area. The “cold” pixel can be selected on a well-irrigated crop surface that completely covers the soil with the vegetation or the surface of a pond. In this case, the “cold” pixel was selected on the surface of a lake. The air temperature near the surface and the surface temperature are considered equal for that pixel. Thus, zero value was assumed for the sensible heat flux (H) and the maximum latent heat flux was determined. The “hot” pixel was selected in a dry farming field, with soil exposed or without vegetation, where the zero value was considered for the latent heat flux (LE) and thus, maximum sensible heat flux was obtained [9, 18].

The correlation coefficients a and b were used with the aid of the anchor pixels to obtain dT in each pixel. Because in the cold pixel dT = 0, that is, there is a system

with two equations and two unknowns, which enabled the calculation of a and b and then the initial sensible heat flux (H_{initial}) was obtained. The next step was to consider the condition of atmospheric stability, making corrections in the values of H in the iterative process. Therefore, the Monin-Obukhov similarity theory (L, in m) was applied to know the stability condition of the atmosphere, that is, whether it is unstable ($L < 0$), stable ($L > 0$) or neutral ($L = 0$). In sequence, through the formulations suggested by Allen et al. [9]), it was possible to obtain the values of the stability corrections for the transport of momentum (ψ_m) and sensible heat (ψ_h) and the friction velocity (u^*) was estimated considering the atmospheric condition [9, 18]:

$$u_* = \frac{k u_{100}}{\ln\left(\frac{z}{z_{0m}}\right) - \psi_{m(100m)}}$$

By using the corrected value of u^* , the aerodynamic drag (r_{ah}) corrected for the stability conditions of the atmosphere was obtained:

$$r_{ah} = \frac{\ln\left(\frac{z_2}{z_1}\right) - \psi_{h(2m)} + \psi_{h(0.1m)}}{u_* k}$$

After that, the temperature difference function (dT) was recalculated by repeating the procedures mentioned above until stability in the successive values of dT and r_{ah} for the hot pixel was observed. Finally, the latent heat flux (LE) was obtained as a residue of the classical equation of the energy balance.

The components of the energy balance were used to estimate the evaporative fraction (λ) [9, 10]:

$$\lambda = \frac{LE}{LE + H} = \frac{LE}{Rn - G}$$

The evaporative fraction was used to estimate plant biomass. For this purpose, the photosynthetically active radiation (PAR, $W m^{-2}$) and the fraction of the intercepted PAR (F_{PAR} , $W m^{-2}$) were estimated using the equations [11]:

$$PAR = 0.48 K_{daily}^{\downarrow}$$

$$F_{PAR} = -0.161 + 1.257 NDVI$$

Where, K_{daily}^{\downarrow} is the incident solar radiation on a daily scale, given in $W m^{-2}$.

After the estimation of PAR and F_{PAR} , PAR absorption by vegetation ($APAR$, $W m^{-2}$) can be determined using the equation [11]:

$$APAR = F_{PAR} \times PAR$$

At this point, when the scalar water availability (W) was replaced in the model proposed by Field et al. [14]. By the evaporative fraction (λ , [19]) it was possible to estimate the efficiency of the use of radiation (ε_f) by:

$$\varepsilon_f = \varepsilon_f^* T_1 T_2 \lambda$$

Where, ε_f^* is the maximum efficiency of the use of the radiation, equal to $2.5 g MJ^{-1}$ [20, 21]; and T_1 and T_2 are temperature scales. Afterward, the above-ground plant biomass was obtained through the model proposed by Monteith [14] and applied by Bastiaanssen and Ali [11] and Teixeira et al. [22]:

$$Bio = \varepsilon_f (APAR(t))$$

Where Bio is the plant biomass in the period t ($kg m^{-2}$).

III. RESULTS AND DISCUSSION

Figure 2A shows the estimated albedo map for the pasture areas of the Experimental Farm of Embrapa Beef Cattle. It is observed that the albedo was higher than 0.35 in pixels of the image highlighted in orange and red, probably in places with soil exposure, dry vegetation or post-grazing period (residual grass). On the other hand, albedo values in green shades, ranging from 0.21 to 0.28, are located in areas of wet (darker) soils or better vegetation vigor. Andrade et al. [23] obtained, for cultivated pasture area, an average albedo value of 0.225. However, in places of soil exposure or dry vegetation, albedo values between 0.30 and 0.40 were observed. In a study of Moura et al. [24], in pasture areas in the Amazon region, values of average albedo hours of 0.197 and 0.204 were observed for the rainy and dry seasons, respectively.

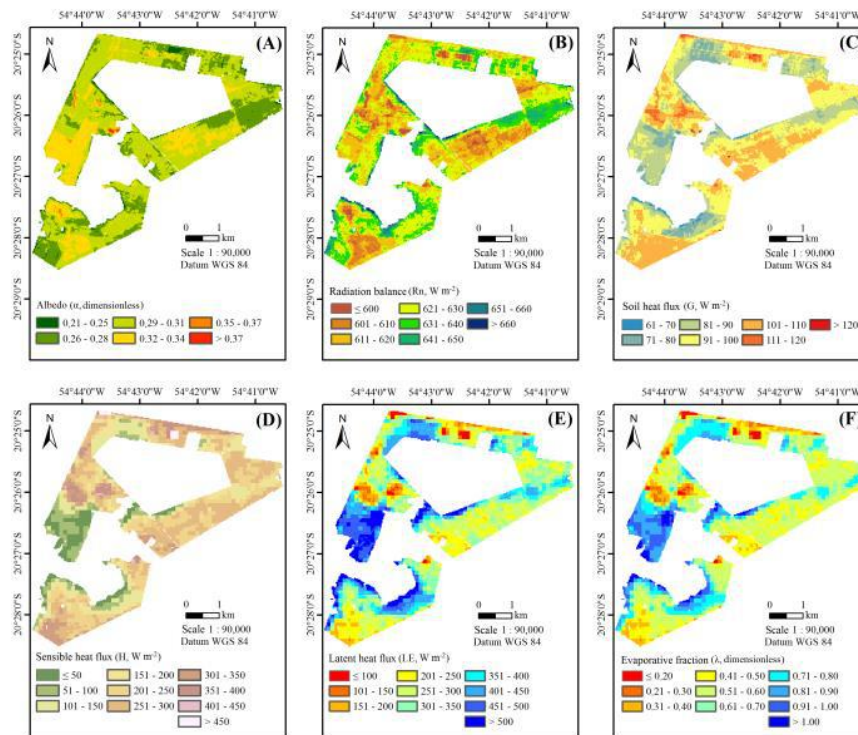


Fig. 2. Visualization of the maps generated from the application of the SEBAL algorithm and TM – Landsat 5 to estimate: (A) albedo (α , dimensionless), (B) radiation balance (R_n , $W m^{-2}$), (C) soil heat flux (G , $W m^{-2}$), (D) sensible heat flux (H , $W m^{-2}$), (E) latent heat flux (LE , $W m^{-2}$) and (F) evaporative fraction (λ , dimensionless) of the pasture areas of the Experimental Farm of Embrapa Beef Cattle, Campo Grande, state of Mato Grosso do Sul, Brazil.

The radiation balance (R_n) of pasture areas, in most of the area, varied between 610 and 650 $W m^{-2}$ (Figure 2B). However, significant spots of $R_n \leq 600 W m^{-2}$ were found in pasture areas with a predominance of exposed soil or water deficit and values of $R_n > 660 W m^{-2}$ in areas of dense vegetation and with no water restrictions. In a study by Santos et al. [25] in the Amazonian biome using MODIS images and SEBAL algorithm combined with data of micrometeorological tower in the pasture area, obtained R_n values for the geographic location of the tower varying from 475.10 $W m^{-2}$ to 599.44 $W m^{-2}$.

In relation to the soil (G , Figure 2C), sensible (H , Figure 2D) and latent (LE , Figure 2E) soil heat fluxes, it was found that pasture areas with water deficit or soil exposure showed, as expected, higher components of G and H and lower for LE . However, an inverse condition was observed when analyzing these components of energy fluxes in pasture areas with dense vegetation or with no water restrictions. In this case, it was found values of $G \leq 90 W m^{-2}$, $H \leq 150 W m^{-2}$ and $LE > 350 W m^{-2}$. By using the Bowen's ratio method, Biudes et al. [26] observed that, on average, pasture areas had LE of 319.7 $W m^{-2}$ and 259.7 $W m^{-2}$ in rainy and dry seasons, respectively. For the H component, the authors observed the average values of 239.4 $W m^{-2}$ and 159.3 $W m^{-2}$, for rainy and dry seasons, respectively. In relation to the heat flux in the soil (G), Biudes et al. [26] verified average values of 41.4 $W m^{-2}$ and 37.6 $W m^{-2}$ in rainy and dry

seasons, respectively. In our study, values of G predominated in the range of 61 $W m^{-2}$ to 120 $W m^{-2}$. In this case, Galeano et al. [27] estimated the maximum value of G within this range of variation (106.4 $W m^{-2}$).

Figure 2F shows the evaporative fraction (λ , dimensionless) estimated for pasture areas. It is observed that the greater evaporative fraction of pasture areas is represented in shades of blue ($\lambda > 0.70$). According to Figures 3A and 3B, vegetation indices ($NDVI \geq 0.5$ and $IAF \geq 2.0 m^2 m^{-2}$) indicate good vegetation development in these areas. For pasture areas, Rubert et al. [28] observed an annual average value of the evaporative fraction of 0.71, with minimum and maximum values of 0.54 and 0.89, respectively.

Figure 3C shows the map of the biomass availability estimate (Bio, kg/ha) of the pasture areas after the application of the SEBAL algorithm and TM – Landsat 5 image. It is observed that on pastures with the predominance of exposed soil (brown class) the Bio was below 1000 $kg ha^{-1}$. On the other hand, in some pasture areas, represented on the map in shades of blue, the Bio was above 7000 $kg ha^{-1}$. Barbosa et al. [29] obtained a biomass availability of *Panicum maximum* cv. Mombaça of 7200 $kg ha^{-1}$ in the summer and 2400 $kg ha^{-1}$ in winter. Carnevali [30] analyzed the availability of this forage in pre- and post-grazing submitted to combinations of grazing intensities and frequencies in rotational stocking observed variation between 4300 and 8900 $kg ha^{-1}$ in pre-

grazing. Nevertheless, the observed values oscillated between 1400 and 4920 kg ha⁻¹ in the post-grazing according to the height of the residue and time of year. In a study carried out by Iwamoto et al. [31] to evaluate the production of Tanzania grass under different nitrogen rates and discontinuous grazing, biomass availability at the highest dose (450 kgN ha⁻¹) was 2970, 4160 and 4600 kg ha⁻¹ in the fall, spring and summer, respectively. Even

so, Yet, Barbosa [15] studied the Tanzania grass in the Experimental Farm of the Embrapa Gado de Corte, obtained biomass availability ranging from 3650 to 7490 kg ha⁻¹ in the pre-grazing. However, in the post-grazing, the observed values varied between 2000 and 4300 kg ha⁻¹, according to the height of the residue and time of the year.

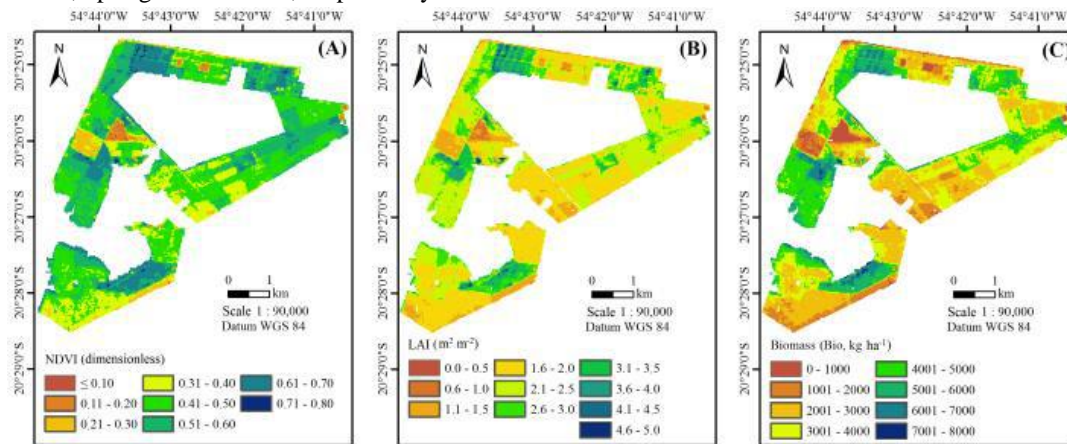


Fig. 3. Visualization of the maps generated from the application of the SEBAL algorithm and TM – Landsat 5 to estimate: (A) normalized difference vegetation index (NDVI, dimensionless), (B) leaf area index (LAI, m² m⁻²) and (C) aboveground plant biomass (Bio, kg ha⁻¹) of the pasture areas of the Embrapa Experimental Beef Cattle Farm, Campo Grande, state of Mato Grosso do Sul.

Figure 4 shows the comparison of the average biomass availability data observed by Barbosa [15] together with the average data estimated with the aid of SEBAL and TM – Landsat 5 images for experimental pasture area in 15 pickets with Tanzania grass in 6 treatments (25/100; 25/95; 50/100; 50/95 and 50/90) in intensity combinations (residues from 25 to 50 cm) and frequencies (90, 95 and 100% light intercepted by the canopy) of monitored defoliation based on the predetermined condition of the canopy structure over the evaluation period. The average value observed for the 15 pickets with Tanzania grass was 4009 kg ha⁻¹. However, the average value was estimated at 3689 kg ha⁻¹, with an average difference between the observed and estimated values of 320 kg ha⁻¹ (8.68%) (Figure 4). Figure 5 shows that the estimated average values had a coefficient of determination (R²) of 0.7108. In this case, the adjustment between the observed and estimated average data is considered reasonable.

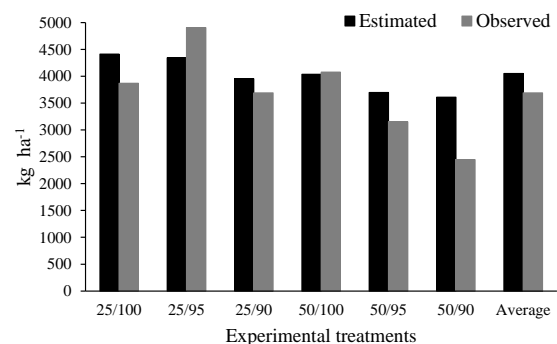


Fig. 4. Average biomass data (kg ha⁻¹) observed and estimated for the 15 pickets with Tanzania grass under different treatments (residue/ light interception: 25/100; 25/95; 25/90; 50/100; 50/95 and 50/90 – according to Barbosa [15]).

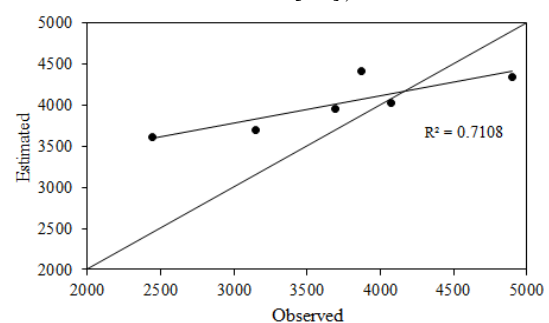


Fig. 5. Visualization of the adjustment between the observed and estimated average biomass data (kg ha⁻¹).

It should be emphasized that, in complementary studies, it is interesting to use high spatial resolution images (such as Geoeye, Rapideye, Worldview, among others) for estimating the biomass and thus to evaluate the adjustment between the observed and the estimated data. However, since these images do not have a thermal band for SEBAL application, the SAFER (*Surface Algorithm For Evapotranspiration Retrieving*) algorithm appears as one of the alternatives [22]. It is worth mentioning that there is also the possibility of using Unmanned Aerial Vehicle (UAV), which can be boarded with cameras for the imaging of surface targets in visible (RGB), near-infrared (NIR) and thermal bands, generating data in which the algorithms and models can be later applied to extract information of the targets of interest with very high spatial and temporal resolution, for example, in the estimation and monitoring of the biomass and hydric conditions of pastures on a picket scale.

IV. CONCLUSION

In general, it is concluded that the application of remote sensing techniques associated with models and algorithms, appears as a relevant alternative for estimation of biophysical parameters and indicator of forage availability in different time and space scales. These geotechnical tools also stand out for the possibility of performing several types of monitoring that can assist the farmer in making decisions regarding the planning and management of the extensive production of beef cattle and milk, taking into account, for example, analyses of indicators related to the economic and environmental sustainability of pasture areas.

REFERENCES

- [1] Vilela, L.; Martha Junior, G. B.; Macedo, M. C. M.; Marchão, R. L.; Guimarães Júnior, R.; Pulrolnik, K.; Maciel, G. A. (2011). Sistemas de integração lavoura-pecuária na região do Cerrado. Pesquisa Agropecuária Brasileira, 46 (10), pp. 1127-1138. <https://dx.doi.org/10.1590/S0100-204X2011001000003>
- [2] Andrade, R. G.; Teixeira, A. H. C.; Leivas, J. F.; Nogueira, S. F. (2016). Analysis of evapotranspiration and biomass in pastures with degradation indicatives in the Upper Tocantins River Basin, in Brazilian Savanna. Revista Ceres, 63, pp. 754-760.
- [3] Dias-Filho, M. B. (2016). Degradação de pastagens: processos, causas e estratégias de recuperação. 4. ed. rev., atual. e ampl. Belém, PA.
- [4] DIEESE (2011). Estatísticas do meio rural 2010-2011. 4. ed. São Paulo: DIEESE: NEAD: MDA.
- [5] Dias-Filho, M. B. (2014). Diagnóstico das pastagens no Brasil. Belém, PA: Embrapa Amazônia Oriental, 36 p. (Documentos / Embrapa Amazônia Oriental, ISSN 1983-0513; 402).
- [6] Grigera, G.; Oesterheld, M.; Pacín, F. (2007). Monitoring forage production for farmers' decision making. Agricultural Systems, 94 (3), pp.637-648.
- [7] Bastiaanssen, W. G.M.; Menenti, M.; Feddes, R. A.; Holtslag, A. A. M. (1998a). A remote sensing surface energy balance algorithm for land (SEBAL) 1. Formulation. Journal of Hydrology, 212-213, pp.198-212.
- [8] Bastiaanssen, W. G. M.; Pelgrum, H.; Wang, J.; Ma, Y.; Moreno, J. F.; Roerink, G. J.; Van der Wal, T. (1998b). A remote sensing surface energy balance algorithm for land (SEBAL): 2. Validation. Journal of Hydrology, 212-213, pp.213-229.
- [9] Allen, R.; Tasumi, M.; Trezza, R. (2002). SEBAL (Surface Energy Balance Algorithms for Land) – Advanced Training and Users Manual – Idaho Implementation, version 1.0, 98p.
- [10] Andrade, R. G.; Sediya, G. C.; Paz, A. R.; Lima, E. P.; Facco, A. G. (2012). Geotecnologias aplicadas à avaliação de parâmetros biofísicos do Pantanal. Pesquisa Agropecuária Brasileira, 47 (9), pp. 1227-1234.
- [11] Bastiaanssen, W. G. M.; Ali, S. (2003). A new crop yield forecasting model based on satellite measurements applied across the Indus Basin, Pakistan. Agriculture Ecosystems & Environment, 94, pp.321-340.
- [12] Samarasinghe, G. B. (2003). Growth and yields of Sri Lanka's major crops interpreted from public domain satellites. Agricultural Water Management, 58, pp. 145-157.
- [13] Monteith, J. L. (1972). Solar radiation and productivity in tropical ecosystems. Journal of Applied Ecology, 9, pp. 747-766.
- [14] Field, C. B., Randerson, J. R., Malmström, C. M. (1995). Global net primary production: combining ecology and remote sensing. Remote Sensing of Environment, 51, pp. 74-88.
- [15] Barbosa, R. A. (2004). Características morfofisiológicas e acúmulo de forragem em capim-Tanzânia (*Panicum maximum* Jacq. Cv. Tanzânia) submetido a frequências e intensidades de pastejo. Viçosa, MG: UFV. 116p. Tese (Doutorado em Zootecnia) – Universidade Federal de Viçosa.
- [16] Bastiaanssen, W. G. M. (2000). SEBAL – based sensible and latent heat fluxes in the irrigated Gediz Basin, Turkey. Journal of Hydrology, 229, pp.87-100.
- [17] Silva, B. B.; Bezerra, M. V. C. (2006). Determinação dos fluxos de calor sensível e latente na superfície utilizando imagens TM - Landsat 5. Revista Brasileira de Agrometeorologia, 14 (2), pp. 174-186.

- [18] Andrade, R. G. (2013). Evapotranspiração por Sensoriamento Remoto. In: Antônio Roberto Pereira, Gilberto Chohaku Sedyama, Nilson Augusto Villa Nova. (Org.). Evapotranspiração. 1a ed. Campinas, SP: FUNDAG, pp. 271-300.
- [19] Crago, R. D. (1996). Conservation and variability of the evaporative fraction during the daytime. *Journal of Hydrology*, 180, pp. 173-194.
- [20] Kiniry, J. R.; Tischler, C. R.; Van Esbroeck, G. A. (1999). Radiation use efficiency and leaf CO₂ exchange for diverse C₄ grasses. *Biomass and Bioenergy*, 17, pp. 95-112.
- [21] Gómez, S.; Guenni, O.; Bravo de Guenni, L. (2012). Growth, leaf photosynthesis and canopy light use efficiency under differing irradiance and soil N supplies in the forage grass *Brachiaria decumbens* Stapf. *Grass and Forage Science*, 68, pp. 395-407.
- [22] Teixeira, A. H. de C.; Scherer-Warren, M.; Hernandez, F. B. T.; Andrade, R. G.; Leivas, J. F. (2013). Large-Scale Water Productivity Assessments with MODIS Images in a Changing Semi-Arid Environment: A Brazilian Case Study. *Remote Sensing*, 5, pp. 5783-5804.
- [23] Andrade, R. G.; Batistella, M.; Amaral, T. B.; Menezes, S. J. M. C. (2009). Estimativa do Albedo em áreas de pastagem e floresta no Mato Grosso do Sul. In: Congresso Brasileiro de Agroinformática, 7., Viçosa, MG. Anais... Viçosa, MG: SBIAgro/UFV, 2009. 5p.
- [24] Moura, M. A. L., Lyra, R. F. F., Benincasa, M., Souza, J. S., Nascimento Filho, M. F. (1999). Variação do albedo em áreas de floresta e pastagem na amazônia. *Revista Brasileira de Agrometeorologia*, 7 (2), pp. 163-168.
- [25] Santos, C. A. C.; Wanderley, R. L. N.; Araújo, A. L.; BEZERRA, B. G. (2014). Obtenção do saldo de radiação em áreas de pastagem e floresta na Amazônia (estação seca) através do sensor Modis. *Revista Brasileira de Meteorologia*, 29 (3), pp. 420-432.
- [26] Biudes, M. S.; Campelo Júnior, J. H.; Nogueira, J. S.; Sanches, L. (2009). Estimativa do balanço de energia em cambarazal e pastagem no norte do Pantanal pelo método da razão de Bowen. *Revista Brasileira de Meteorologia*, 24 (2), pp. 135-143.
- [27] Galeano, D. C.; Biudes, M. S.; Danelichen, V. H. M.; Fabian, F. A.; Souza, M. C. (2013). Energy balance in a pasture in the Pantanal. *Journal of Biotechnology and Biodiversity*, 4 (2), pp. 113-118.
- [28] Rubert, G. C. D.; Roberti, D. R.; Diaz, M. B.; Moraes, O. L. L. (2016). Estimativa da evapotranspiração em área de pastagem em Santa Maria-RS. *Revista Ciência e Natura*, 38, pp. 300-304.
- [29] Barbosa, M. A. A. F., Damasceno, J. C., Cecato, U., Sakaguti, E. S. (1996). Estudo de perfilhamento em 4 cultivares de *Panicum maximum* Jacq. Submetidos à duas alturas de corte. In: Reunião Anual da Sociedade Brasileira de Zootecnia, 33., 1996, Fortaleza, CE. Anais... Fortaleza: SBZ. pp. 109-111.
- [30] Carnevalli, R. A. (2003). Dinâmica da rebrotação de pastos de capim-Mombaça submetidos a regimes de desfolhação intermitente. Piracicaba, SP: ESALQ. 136p. Tese (Doutorado em Agronomia) – Escola Superior de Agricultura “Luiz de Queiroz”, Universidade de São Paulo.
- [31] Iwamoto, B. S., Cecato, U., Ribeiro, O. L., Mari, G. C., Peluso, E. P., Lins, T. O. J. D. A. (2014). Produção e composição morfológica do capim-tanzânia fertilizado com nitrogênio nas estações do ano. *Bioscience Journal*, 30 (2), pp. 530-538.